Journal of *Marine Science and Engineering*

MDPI

Article

Scale Model Experiment on Local Scour around Submarine Pipelines under Bidirectional Tidal Currents

Zhiyong Zhang [1,*], Yakun Guo [2,*], Yuanping Yang [1], Bing Shi [3] and Xiuguang Wu [1]

[1] Zhejiang Institute of Hydraulics and Estuary, Hangzhou 310020, China; yangyp@zjwater.gov.vn (Y.Y.); wuxg@zjwater.gov.cn (X.W.)
[2] School of Engineering & Informatics, University of Bradford, Bradford BD7 1DP, UK
[3] College of Engineering, Ocean University of China, Qingdao 266100, China; bings@ouc.edu.cn
* Correspondence: zhangzy@zjwater.gov.cn (Z.Z.); y.guo16@bradford.ac.uk (Y.G.)

Abstract: In nearshore regions, bidirectional tidal flow is the main hydrodynamic factor, which induces local scour around submarine pipelines. So far, most studies on scour around submarine pipelines only consider the action of unidirectional, steady currents and little attention has been paid to the situation of bidirectional tidal currents. To deeply understand scour characteristics and produce a more accurate prediction method in bidirectional tidal currents for engineering application, a series of laboratory scale experiments were conducted in a bidirectional current flume. The experiments were carried out at a length scale of 1:20 and the tidal currents were scaled with field measurements from Cezhen pipeline in Hangzhou Bay, China. The experimental results showed that under bidirectional tidal currents, the scour depth increased significantly during the first half of the tidal cycle and it only increased slightly when the flow of the tidal velocity was near maximum flood or ebb in the following tidal cycle. Compared with scour under a unidirectional steady current, the scour profile under a bidirectional tidal current was more symmetrical, and the scour depth in a bidirectional tidal current was on average 80% of that under a unidirectional, steady current based on maximum peak velocity. Based on previous research and the present experimental data, a more accurate fitted equation to predict the tidally induced live-bed scour depth around submarine pipelines was proposed and has been verified using field data from the Cezhen pipeline.

Keywords: submarine pipeline; scour; scale model experiment; bidirectional tidal current; unidirectional current

Citation: Zhang, Z.; Guo, Y.; Yang, Y.; Shi, B.; Wu, X. Scale Model Experiment on Local Scour around Submarine Pipelines under Bidirectional Tidal Currents. *J. Mar. Sci. Eng.* **2021**, *9*, 1421. https://doi.org/10.3390/jmse9121421

Academic Editors: José A. F. O. Correia

Received: 8 November 2021
Accepted: 8 December 2021
Published: 12 December 2021

1. Introduction

With the development and exploitation of offshore oil and gas resources, submarine pipelines are widely used to transport oil and gas from offshore to onshore areas. However, in a harsh ocean environment, suspension of submarine pipelines caused by local scour often occurs, leading to instability and breakage of the pipelines.

Local scour around submarine pipelines is a typical scour phenomenon in a marine environment. In past decades, extensive studies have been carried out to investigate the scour mechanism, scouring process and scour protection around submarine pipelines [1–8]. Mao (1986) [9] studied the scour characteristics under a steady current in an experimental flume and discussed the effect of vortices on the onset of scour. Chiew (1990) [10] carried out laboratory experiments to investigate the onset of scour and found that scour around a pipeline could be prevented by placing a plate on the upstream side of the pipeline. Some researchers [11–13] developed various clear-water empirical formulas to predict equilibrium scour depth based on their own experimental data under a steady current, respectively. However previous studies mostly focused only on the clear-water scour conditions (i.e., $u < u_c$, where u is flow velocity and u_c is the critical velocity for sediment incipient motion). For the live bed conditions ($u > u_c$) (Figure 1), the sandy bed outside the scour hole is also eroded due to high flow intensity and sediment is transported into the

scour hole below the pipeline. This makes it more complex than clear-water scour. However, there are only a few studies in the literature [9,14,15] that reported experimental results.

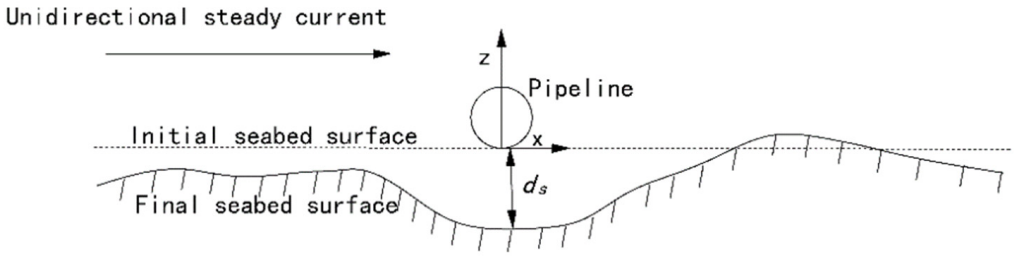

Figure 1. Live-bed scour profile around a submarine pipeline.

The scour around submarine pipeline under waves, combined waves and currents were also paid attention to. Under wave conditions, wake structure occurred on both sides of the pipeline and induced lee-wake erosion on both sides of the pipe [16,17]. The scour depth under the wave action was mainly influenced by the wave period and the maximum velocity. Sumer and Fredsøe (1990) [18] experimentally studied the scour around pipelines under wave action with different Keulegan–Carpenter numbers ($KC = u_{wmax}T_w/D$, u_{wmax}, T_w which are the wave peak velocity and period, respectively, and D is the pipeline diameter) and found that the relative scour depth d_{sm}/D (d_{sm} is the maximum scour depth) is a function of KC^k ($k = 0.5$). Several other relative empirical formulas about KC were also obtained to predict the scour depth caused by waves [19–23]. For wave plus current, scour development has also been investigated by Zhang et al. (2016), Zhang et al. (2017) [24] and Li et al. (2020) [25].

In real nearshore regions, the tidal currents induced by the tidal force of celestial bodies are unsteady, with time varying velocities and flow directions [26,27]. Figure 2 shows a typical time process of tidal average vertical velocities and tidal level from field data from the Cezhen pipeline in Hangzhou Bay, China. It was seen that the flow velocity varied as sinusoids and the flow direction changed bidirectionally, which was similar to waves. However, the tidal period was nearly 12 h, which was much longer than common wave time periods ($T < 100$ s). Time-varying velocity with longer time periods made the tidal current different from steady currents and waves [28]; hence, the scour induced by tidal current was also different from steady currents and waves. However, at present, there is no study on the scour around submarine pipelines under bidirectional tidal currents. In practical engineering, the scour depth under bidirectional tidal flow is predicted by equations under steady currents or waves, which overestimates [29] the scour depth. The objective of this study was to gain further insights into the scour characteristics around submarine pipelines under bidirectional tidal currents. A more accurate equation was also developed to predict the maximum scour depth beneath submarine pipelines for engineering applications.

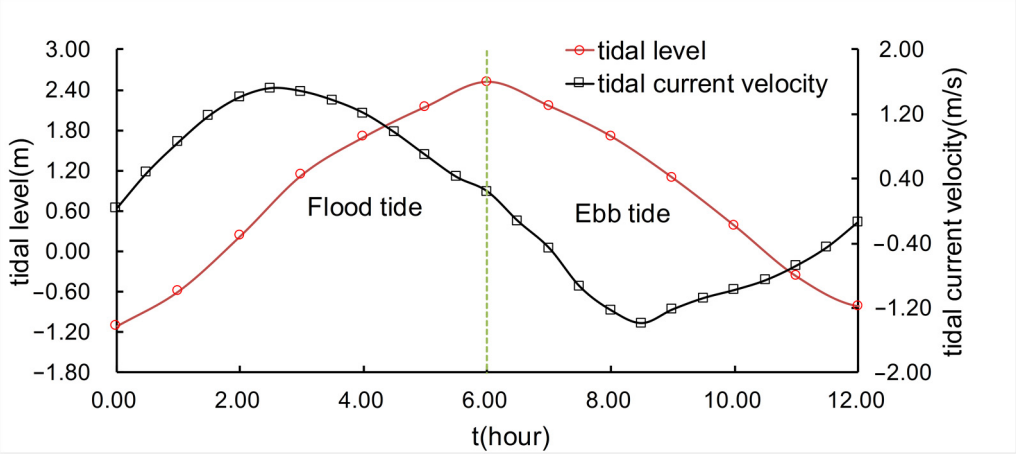

Figure 2. Typical time process of tidal velocity and water level in Hangzhou Bay.

2. Experiment Setup

The laboratory scale model experiments for the scour around submarine pipelines under tidal current were conducted in a flume in the Key Laboratory of Estuary and Coast of Zhejiang Province in China. Figure 3 shows the experimental setup with top and side views. The flume was 50 m in length, 4 m in width and 0.5 m in depth. There were eight reversal pumps at both sides of the flume and the bidirectional tidal current could be generated using a multi-pump frequency control system. There was a sand basin (4.0 m × 4.0 m × 0.2 m) placed in the middle of the flume (see Figure 3). The sand basin was filled with sand with a median diameter d_{50} = 0.15 mm, density ρ_s = 2650 kg/m^3 and angle of repose 32°. According to the critical Shields parameter of sediment and the logarithmic form of the velocity profile, the critical velocity for sediment incipient motion was calculated u_c = 0.28 m/s. The diameter (D) of the modeled pipeline was 0.045 m, which was scaled down from the Cezhen pipeline (D = 0.9 m) in Hangzhou Bay, China, with a scaling factor of 1:20. In addition, another pipeline with D = 0.075 m was also used. A Cartesian coordinate system was established with the origin being the contact point of the pipeline and sand bed at the central line. An ADV (acoustic Doppler velocimetry) was used to measure the flow velocity upstream of pipeline. Additionally, there was a camera recording the pictures of the scour profile at regular intervals and the data of the scour profiles were acquired from the pictures using image recognition. This method was also compared with traditional depth probes and showed an accuracy of 1 mm.

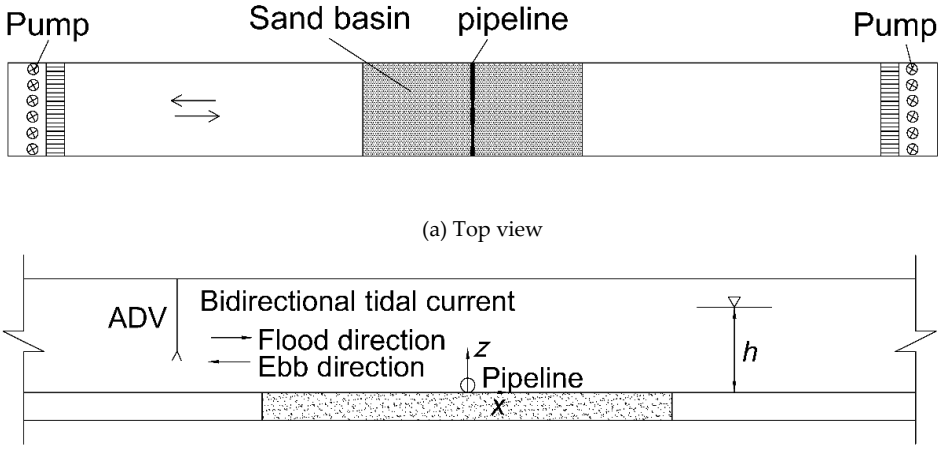

(a) Top view

(b) Side view

Figure 3. Experiment setup: (**a**) top and (**b**) side view.

Experimental runs were carried out under bidirectional tidal current and unidirectional current conditions, respectively. Considering the characteristics of the stronger flow in Hangzhou Bay, the live-bed unidirectional current conditions ($u > u_c$) were studied in the experiment. Details of the experimental flow conditions are listed in Table 1. According to Froude's law, the length scale between the model experiment and prototype was 1:20, and the time scale between the laboratory experiment and the prototype was 1:4.47. Therefore, the period of tidal current in the laboratory experiments was 2.68 h, corresponding to the period of 12 h in the prototype. The tidal current in the experiment was simplified as a regular sinusoid tide:

$$u_t = u_{\max} \sin(2\pi t/T) \quad (1)$$

where u_t is tidal velocity at time t, $u_{\max}$ is the maximum tidal velocity during the flood and ebb phases and T is tidal period. Considering the varying tidal velocity, root mean square velocity u_r was also calculated as effective flow intensity, and for the sinusoidal form of the tidal velocity, u_r could be estimated by $u_r = 2u_{\max}/\pi$.

Table 1. Parameters of the experiments for unidirectional and bidirectional tidal currents.

Test	Pipe Diameter D (m)	Water Depth h (m)	u_0 (m/s)	$u_{\max}$ (m/s)	u_0/u_c or $u_{\max}/u_c$	Root Mean Velocity u_r (m/s)	Maximum Scour Depth d_{sm} (m)
Uni01	0.045	0.30	0.30		1.07	0.30	0.034
Uni02	0.045	0.30	0.35	-	1.25	0.35	0.038
Uni03	0.045	0.30	0.40	-	1.43	0.40	0.046
Uni04	0.045	0.30	0.45		1.61	0.45	0.050
Uni05	0.045	0.30	0.50	-	1.79	0.50	0.054
Uni06	0.075	0.30	0.30		1.07	0.30	0.051
Uni07	0.075	0.30	0.40	-	1.43	0.40	0.068
Uni08	0.075	0.30	0.50	-	1.79	0.50	0.078
Tide01	0.045	0.30	-	0.30	1.07	0.19	0.024
Tide02	0.045	0.30	-	0.35	1.25	0.22	0.034
Tide03	0.045	0.30	-	0.40	1.43	0.25	0.038
Tide04	0.045	0.30	-	0.45	1.61	0.29	0.041
Tide05	0.045	0.30	-	0.50	1.79	0.32	0.043
Tide06	0.075	0.30	-	0.30	1.07	0.19	0.045
Tide07	0.075	0.30	-	0.40	1.43	0.25	0.058
Tide08	0.075	0.30	-	0.50	1.79	0.32	0.066

Figure 4 shows the time history of the simulated flow velocity generated by a multi-pump frequency control system and the theoretical velocity calculated by Equation (1) for $u_{\max}$ = 0.4 m/s. The time history of the experimentally generated tidal velocity was in good agreement with the theoretical value, indicating that the multi-pump frequency control system could generate an excellent bidirectional tidal current.

For the unidirectional current, the flow was kept at constant velocity and depth. The unidirectional velocity u_0 was equal to the maximum peak velocity $u_{\max}$ in a tide period and the water depth was also equal to the value of the bidirectional tidal current (see Table 1 for details of the experimental runs).

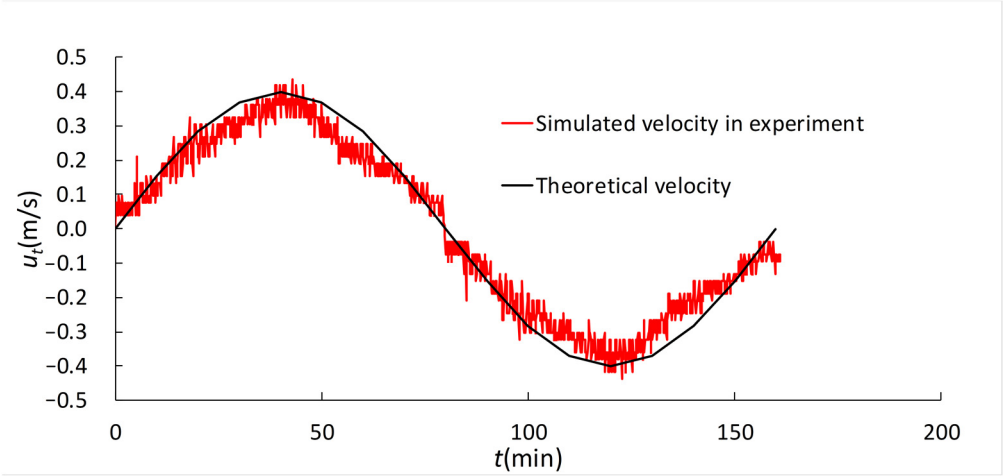

Figure 4. Time history of simulated bidirectional tidal current velocity.

3. Result and Discussion

3.1. Scouring Process and Scour Profile

For the bidirectional tidal current, the reversal flow made the scour process more complicated than that under the unidirectional tidal current. Figure 5 shows the camera images of the scour profiles at different time instants for Tide 01: u_{max} = 0.3 m/s, D = 0.045 m. As seen from the figure, in the first tidal half cycle ($t < 0.5\ T$) (Figure 5a,b), the scour hole below the pipeline developed rapidly and there was a dune downstream of the pipeline, which gradually moved downstream with time. This phenomenon was similar to that under a unidirectional current. However, during the second half tidal cycle ($0.5\ T < t < 1.0\ T$) (Figure 5c,d) with negative flow direction, the sediment in the scour hole was transported out and formed another dune upstream of the pipeline induced by ebb flow, which made the scour profile at $t = 1.0\ T$ (Figure 5d) more symmetric around the pipeline. In the following tidal cycle, $1.0\ T < t < 2.0\ T$ (Figure 5e–h), it could be observed from the figures that the size of the dunes on both sides had a distinct fluctuation, whereas the scour hole below the pipeline and the maximum scour depth exhibited a creeping development. Moreover, by comparing the scour profiles at $t = 3.0\ T$ (Figure 5i) and $t = 10.0\ T$ (Figure 5j), there was no significant change in the scour hole (nearly 19 h). This implied that the scour profile at $t = 3.0\ T$ could be recognized as a dynamic equilibrium scour profile.

To make readers clearly understand the distinction of scour profiles in different currents, the final equilibrium scour profiles for $u_0 = u_{max}$ = 0.3 m/s, 0.4 m/s and 0.5 m/s are plotted in Figure 6, respectively. As detailed in Figure 6, there were two significant differences of scour profiles between the unidirectional and bidirectional currents. The first one is that there was only one dune downstream of the pipeline for the unidirectional steady current, whereas there were two dunes for the bidirectional tidal current and the scour profile was more symmetric. Moreover, the scour depth and width under the unidirectional current were both larger than those of the bidirectional tidal current. Additionally, with increasing velocity the size of the scour hole, including scour depth and width, also both increased.

3.2. Temporal Development of Scour Depth

In practical engineering, significant attention is paid to the maximum scour depth of the pipeline by engineers because it influences the submarine pipeline design and scour protection. Figure 7 shows the temporal development of the normalized scour depth (ds/D) at $x = 0.0\ D$ versus dimensionless time t/T (T is tidal period) for various tidal currents, and the time history of relative flow velocity u_t/u_{max} is also shown. The figure demonstrated that scour depth increased rapidly during the first half of the tidal cycle. After that, the scour depth only increased slightly when the flow was near maximum flood or ebb tidal

velocity and there was no scour development when the flow was close to zero velocity. It could also be seen that the decrease in scour depth induced by sediment backfilling did not obviously occur, which may be ascribed to the fact that the flow was turbulent enough to keep the sediment in suspension longer, allowing it to be transported out of the scour hole.

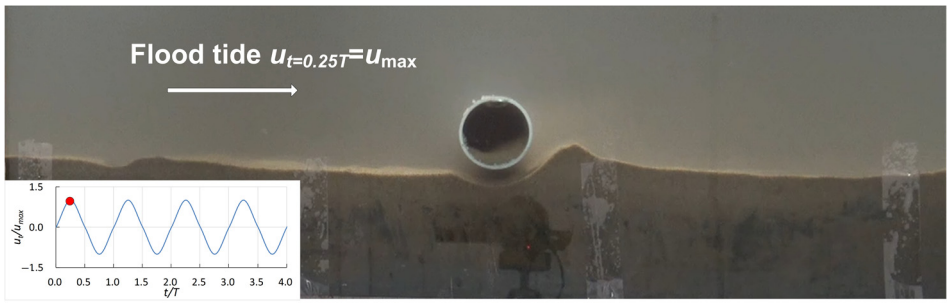

(a)

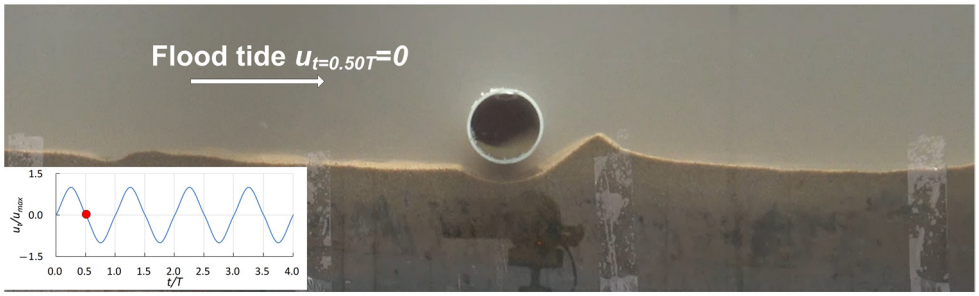

(b)

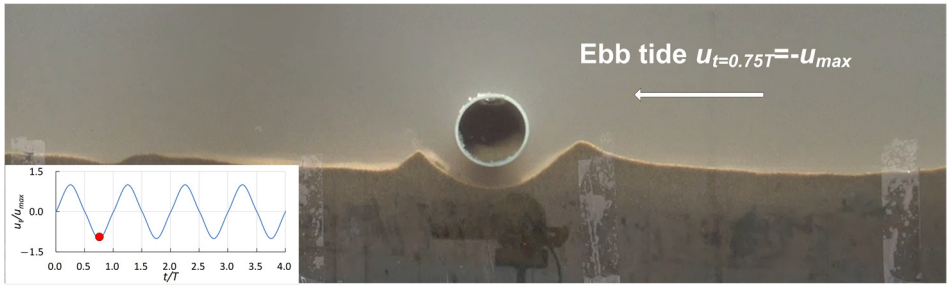

(c)

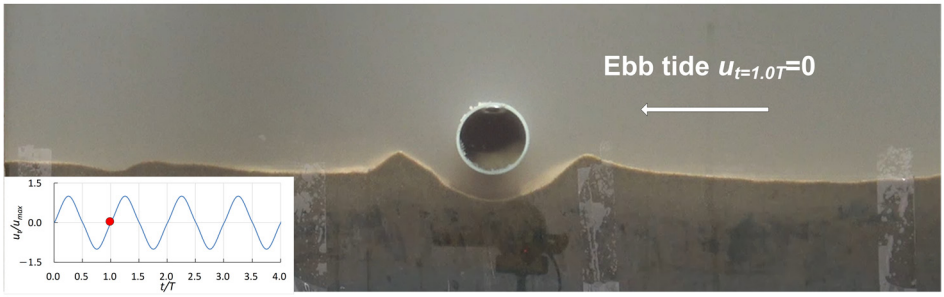

(d)

Figure 5. *Cont.*

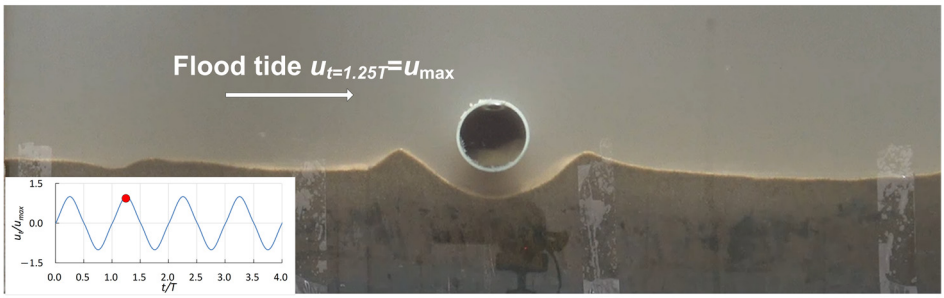

(e)

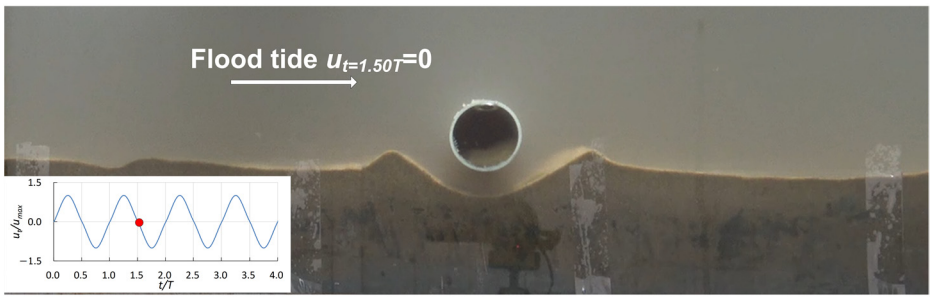

(f)

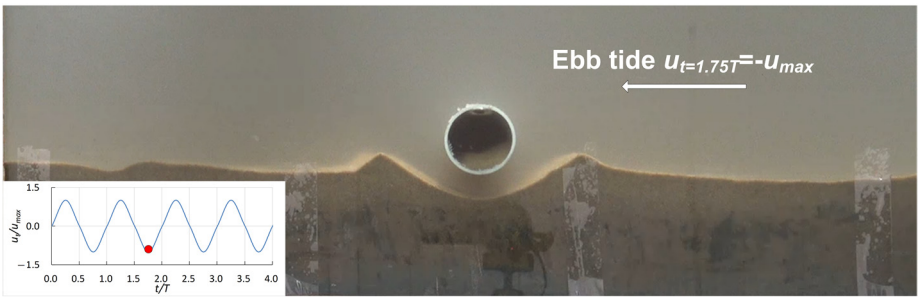

(g)

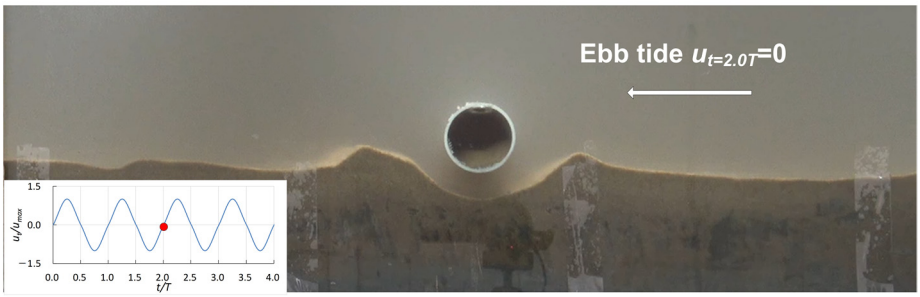

(h)

Figure 5. *Cont.*

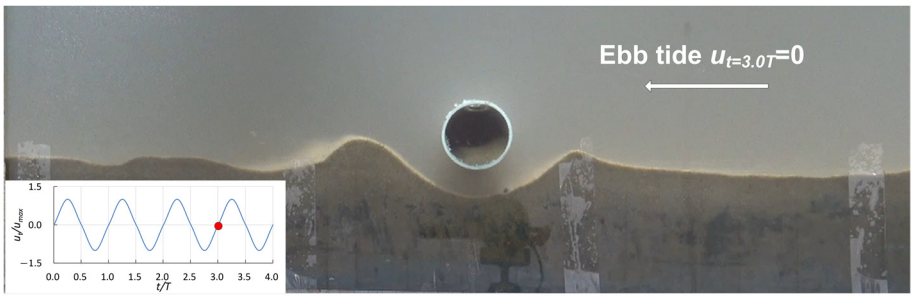

(i)

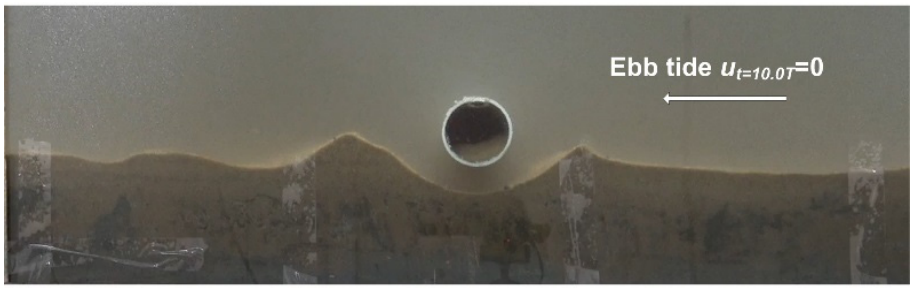

(j)

Figure 5. Time process of scour profile for Tide 01: u_{max} = 0.3 m/s, D = 0.045 m. (**a**) t = 0.25 T; (**b**) t = 0.50 T; (**c**) t = 0.75 T; (**d**) t = 1.0 T; (**e**) t = 1.25 T; (**f**) t = 1.50 T; (**g**) t = 1.75 T; (**h**) t = 2.0 T; (**i**) t = 3.0 T; (**j**) t = 10.0 T.

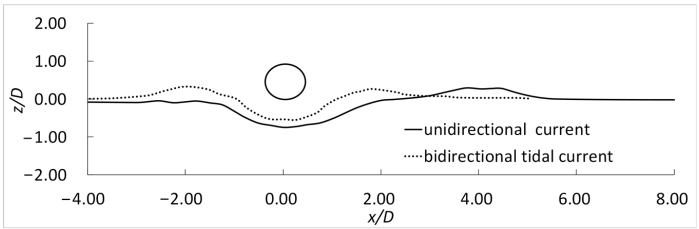

(a)

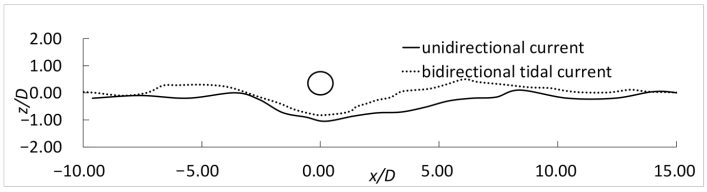

(b)

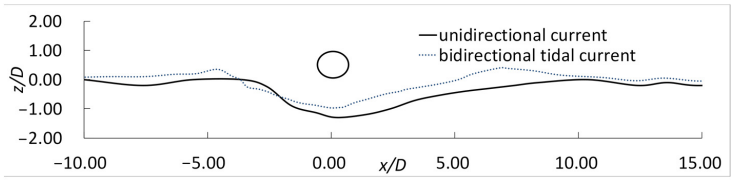

(c)

Figure 6. Comparisons of scour profiles under unidirectional and bidirectional tidal currents. (**a**) $u_0 = u_{max}$ = 0.3 m/s; (**b**) $u_0 = u_{max}$ = 0.4 m/s; (**c**) $u_0 = u_{max}$ = 0.5 m/s.

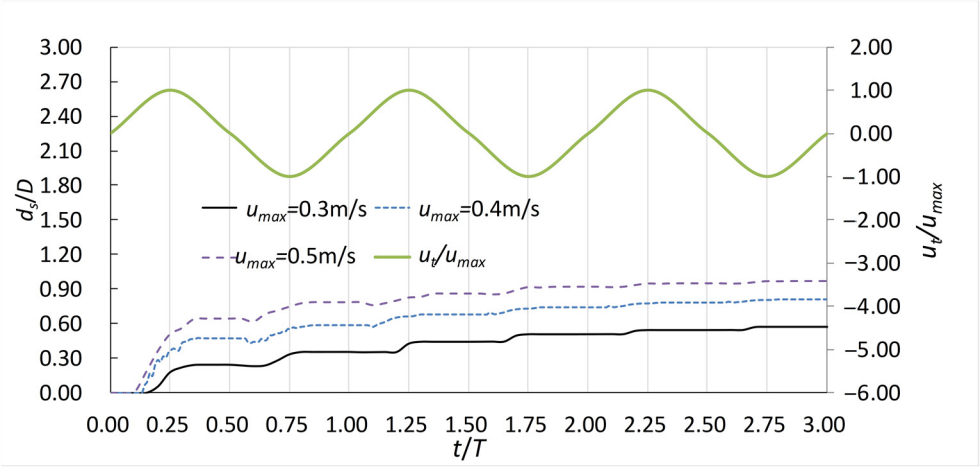

Figure 7. Time development of scour depth under bidirectional tidal currents.

Figure 8 also compares the scour depth development over time under unidirectional and bidirectional tidal currents (u_0 or u_{max} = 0.3 and 0.4 m/s). It was evident that the scour depth development was much slower for the bidirectional tidal current compared to that under unidirectional steady current, whose velocity equaled the maximum velocity of the tide. This implied that the effective flow intensity, u_r, under bidirectional tidal currentd with varied flow velocity was smaller than that of the unidirectional steady current based on u_{max}.

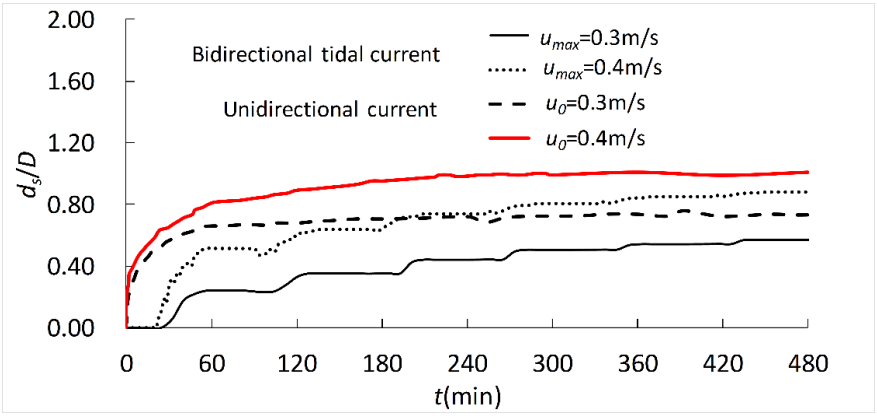

Figure 8. Temporal development of scour depth under bidirectional and unidirectional currents.

3.3. Maximum Scour Depth under Bidirectional Tidal Currents

As reported above, the developments of scour depth under unidirectional and bidirectional tidal currents were different, and hence the final maximum scour depths under different current conditions were also different. Figure 9 shows the dimensional maximum scour depths caused by the bidirectional tidal current and unidirectional steady current, respectively. According to Figure 9, the live-bed scour depth d_{sm} increased with flow velocity, and also increased with pipeline diameter in the same flow conditions. In order to evaluate the difference of maximum scour depth between unidirectional and bidirectional tidal currents, the equilibrium scour depths were transformed to dimensionless values d_{sm}/D (Figure 10). As seen from Figure 10, the maximum scour depths d_{sm}/D at the same flow conditions were nearly the same with different pipeline diameters. Moreover, it was also seen that the maximum scour depth under the bidirectional tidal current d_{sm}/D was smaller than those of the unidirectional current for $u_0 = u_{max}$, and was on average 0.8 times of that of the unidirectional current.

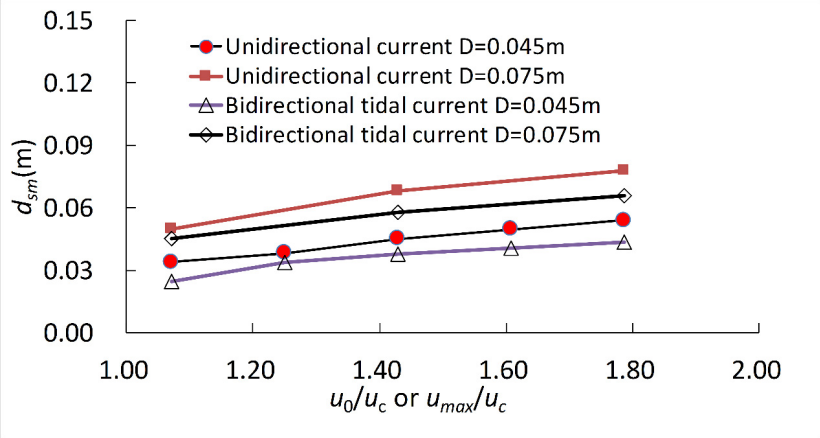

Figure 9. Dimensional maximum scour depth under different flow conditions.

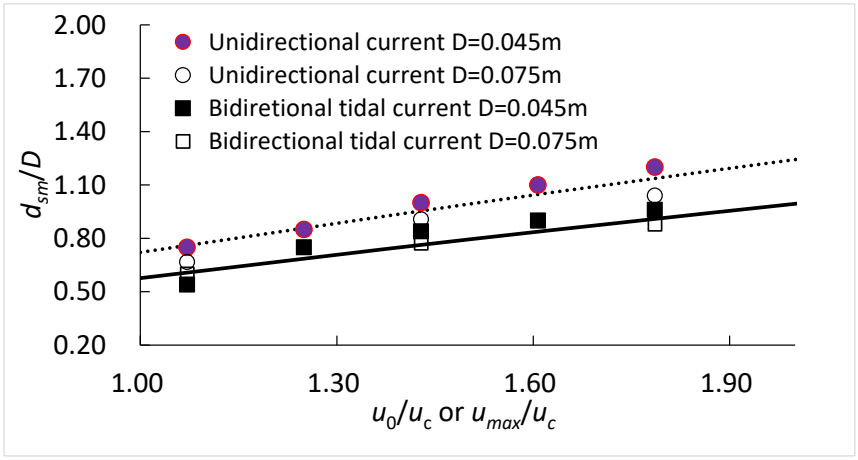

Figure 10. Dimensionless maximum scour depth d_{sm}/D under different flow conditions.

3.4. Prediction of Maximum Scour Depth

According to the present experimental conditions, if the tidal current was regarded as longer time period wave, the *KC* number of each bidirectional tidal current was larger than 300. Sumer and Fredsøe [18] developed a scour depth equation about *KC* under wave and pointed out that when *KC* was larger than 300, the relative scour depth d_{sm}/D was a constant value, 1.73. However, the scour depth of each tidal current case from the present experiment was far less than 1.73, which implied that the scour under the bidirectional tidal current could not be regarded as that under wave.

For the live-bed scour depth around submarine pipelines under unidirectional steady currents, Ibraim and Nalluri [14] studied live-bed scour depths around pipelines based on experiments and established an equation to predict equilibrium scour depth:

$$\frac{d_{sm}}{D} = 0.084\left(\frac{u_0}{u_c}\right)^{-0.3} Fr^{-0.16} + 1.33 \quad (2)$$

where Fr is Froude number, $Fr = u/\sqrt{gh}$.

Sumer and Fredsøe [18] suggested that the maximum scour depth was approximately a constant value:

$$\frac{d_{sm}}{D} = 0.6 \quad (3)$$

Also in practical engineering, except for the above equations, some clear-water scour equations are often used to predict scour depth, even though it is a live-bed condition.

Here a widely used empirical equation by Bijker and Leeuwestein [12] is selected and the equation is as follows:

$$\frac{d_{sm}}{D} = 0.929\left(\frac{{u_0}^2}{2g}\right)^{0.26}\frac{D^{-0.22}}{{d_{50}}^{0.04}} \quad (4)$$

In order to evaluate the accuracy of the above three equations, a total of 46 laboratory experimental data from Mao (1986) [9], Moncada et al. (1999) [15] and the present study were collected. Figure 11 shows the comparisons of experimental measured values and predicted values using Equations (2) and (3). It was found that predicted values by Equation (2) were both greater than 1.33 and were much larger than measured values, which implied that Equation (2) overestimated the live-bed scour depth. Additionally, most of the measured scour depths were larger than 0.6 D which revealed that Equation (3) underestimated the scour depth. The comparisons indicated that the above two predicted equations both have larger errors.

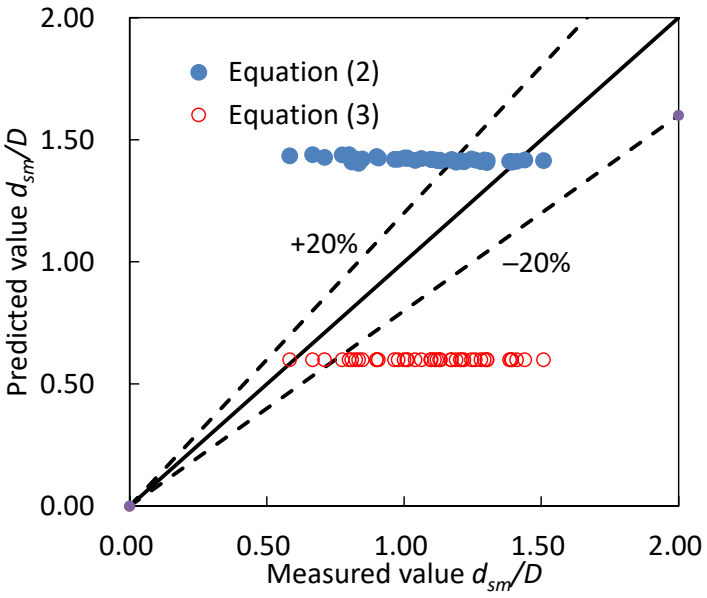

Figure 11. Comparisons of measured and predicted scour depth using Equations (2) and (3).

Figure 12 shows the comparisons between measured scour depths and predicted values by Equation (4). Generally, the measured values were larger than the predicted values which implied that Equation (4) also underestimated the scour depth and had a relative error of 40%. Considering larger errors of the above three equations, it was necessary to develop a more accurate equation. Based on collected experimental data, a new fitted equation with Fr and u_0/u_c was proposed by nonlinear multiple regression (see Equation (5)). Figure 13 shows the comparisons of predicted values using Equation (5) with measured values. It could be seen that the predicted values using Equation (5) were in good agreement with the measured values and the relative error was within 20%. Compared to Equations (2)–(5), it was more suitable for predicting the maximum scour depth of a steady current in live-bed conditions.

$$\frac{d_{sm}}{D} = 1.39\left(\frac{u_0}{u_c}\right)^{0.21} Fr^{0.37} \quad (5)$$

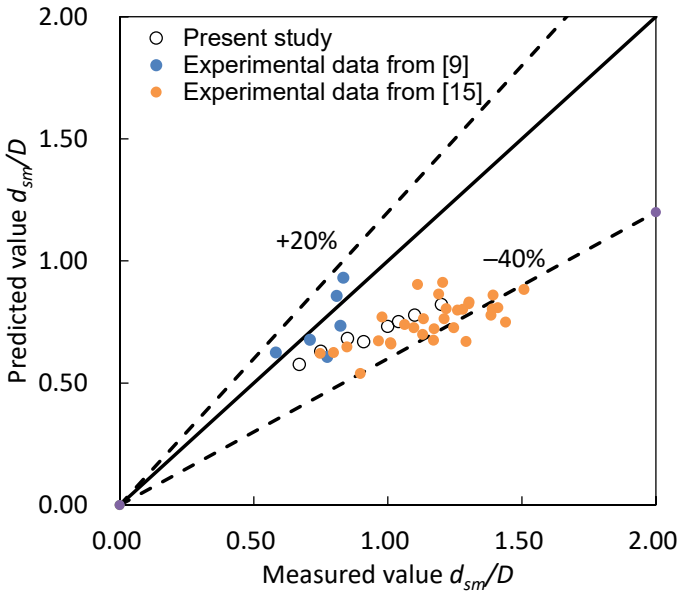

Figure 12. Comparisons of measured and predicted scour depth using Equation (4).

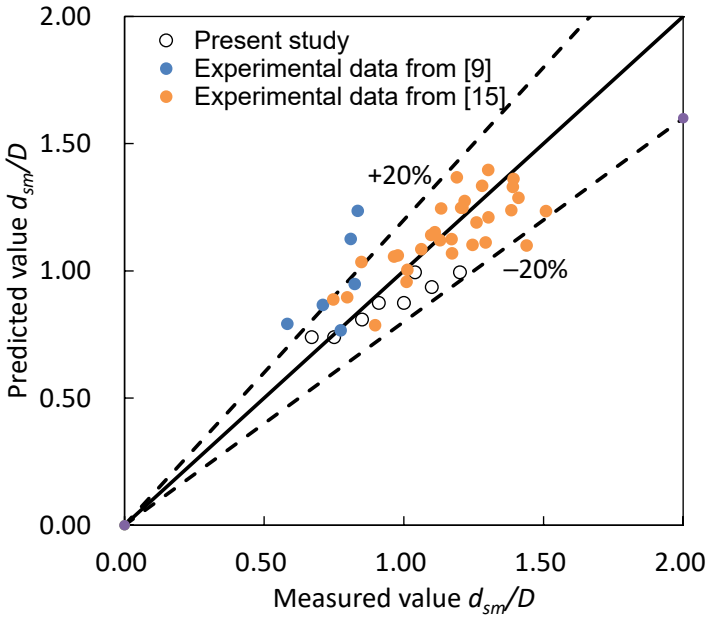

Figure 13. Comparisons of measured and predicted scour depth using Equation (5).

As discussed in 3.3, the maximum scour depth under the bidirectional tidal current was on average 80% of that under the unidirectional steady current. Moreover, considering that a more accurate predicted Equation (5) for scour depth under the steady current has been developed in this study, we can predict the scour depth under the bidirectional tidal current by adding a reduction coefficient (0.8) to Equation (5). Therefore, the maximum live-bed scour depth under the bidirectional tidal current could be calculated as follows:

$$\frac{d_{sm}}{D} = 0.8\left(1.39\left(\frac{u_{\max}}{u_c}\right)^{0.21} Fr^{0.37}\right) = 1.11\left(\frac{u_{\max}}{u_c}\right)^{0.21} Fr^{0.37} \quad (6)$$

Seen from Figure 14, the predicted values using Equation (6) were also in good agreement with the measured values and the relative error was also within 20%.

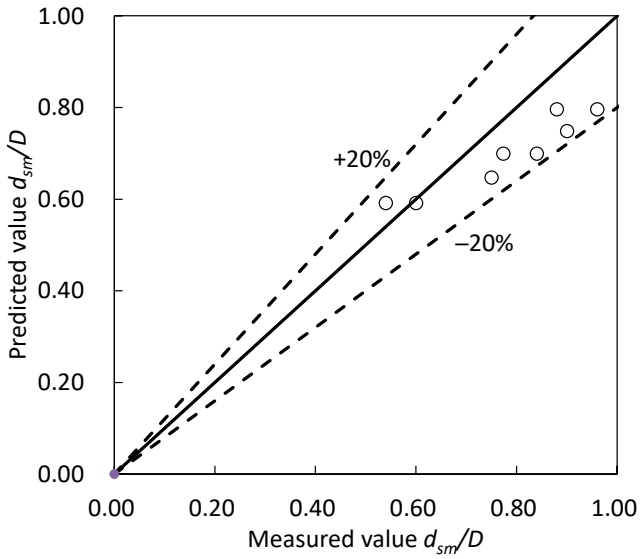

Figure 14. Comparisons of measured and predicted scour depth using Equation (6).

3.5. Comparison with Field Data

As noted above, the maximum scour depth around submarine pipelines had a relationship with the pipeline diameter D, flow velocity (u_{max}), water depth (h) and sediment properties (u_c). However, in practical engineering, the hydrodynamic conditions are larger than in laboratory flow conditions. To accurately predict the scour depth in the field, it is necessary to make sure which equation is more applicable in practical engineering. Consequently, in this study, field data from 2014 from the Cezhen pipeline in tide-dominated Hangzhou Bay were used to validate the predicted equations. According to the field data, there were 15 free span segments mainly located in three regions KP3, KP12 and KP16, and the maximum scour depths of each span segment are listed as follows:

1. KP3: three span segments and maximum scour depths of 0.3 m, 0.4 m and 0.6 m.
2. KP12: four span segments and maximum scour depths of 0.2 m, 0.3 m, 0.4 m and 0.8 m.
3. KP16: eight span segments and maximum scour depths of 0.3 m, 0.2 m, 0.1 m, 0.5 m, 0.2 m, 0.1 m, 0.1 m and 0.2 m.

As seen from above, the maximum scour depths varied largely even with nearly the same conditions in the same region. This may be because some scour depths of the span segments did not develope to dynamic equilibrium scour status, especially the smaller values. Moreover, the maximum values in each region were much closer to the dynamic equilibrium scour status. Consequently, it was reasonable that the maximum values of each region in place of all scour depths of 15 span segments were chosen to validate the scour equation. The dimensionless maximum scour depths of a span segment in each region are shown in Table 2 and the flow conditions of each region are also shown in this table. In addition, the mean sediment size, d_{50}, of the seabed near the pipeline was approximately 0.01 mm and the critical velocity for sediment incipient motion ranged from 0.8 to 1.2 m/s [30] (Table 2), based on a famous fine sediment incipient formula of Zhang et al. [31]. According to the flow and sediment parameters in the field, the maximum scour depths were predicted, respectively, by Equations (3)–(6). Figure 15 shows the predicted values using different equations with field data and Table 3 lists the absolute error (predicted value field data) of each equation. It was shown that the predicted maximum scour depth by Equation (6) was much closer to the field data, with absolute error within 0.1 D, whereas absolute errors using Equations (3) and (4) were 0.04–0.29 D and 0.13–0.38 D, respectively. In addition, it was also found that Equation (4) overestimated the scour values in the field data, while it underestimated the scour values in the experimental data (Figure 12). This may be because Equation (4) was highly sensitive to sediment size

d_{50}, especially smaller values. By evaluating the application of Equation (6) in the field and laboratory experiments, it was validated that Equation (6) was more accurate than the present equations, both in practical engineering and on the laboratory scale.

Table 2. Flow conditions and measured scour depth of the Cezhen pipeline.

Hung Segment Location	Pipeline Diameter D (m)	Water Depth H (m)	Maximum Tidal Velocity u_{max} (m/s)	Sediment Incipient Velocity u_c (m/s)	u_{max}/u_c	Froude Number Fr	Measured Scour Depth d_{sm}/D
KP3	0.9	5.0	1.6	0.8	2.0	0.23	0.67
KP12	0.9	8.0	2.1	1.0	2.1	0.24	0.89
KP16	0.9	10.0	1.8	1.1	1.6	0.18	0.56

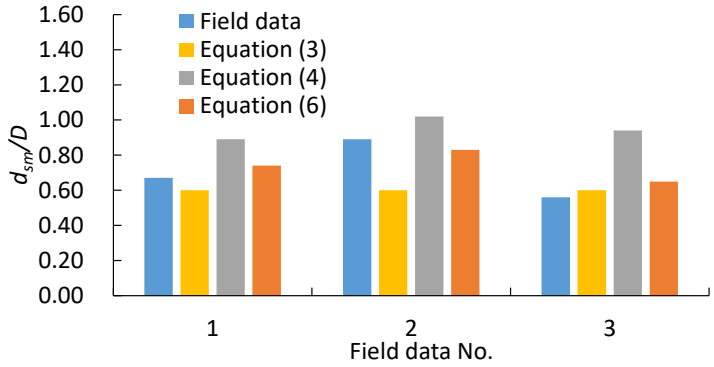

Figure 15. Comparisons of field data and predicted scour depths using different equations.

Table 3. Statistics of predicted error using different equations.

Field Data d_{sm}/D	Equation (6)		Equation (3)		Equation (4)	
	Predicted Value d_{sm}/D	Absolute Error	Predicted Value d_{sm}/D	Absolute Error	Predicted Value d_{sm}/D	Absolute Error
0.67	0.74	0.07	0.60	−0.07	0.89	0.22
0.89	0.83	−0.06	0.60	−0.29	1.02	0.13
0.56	0.65	0.09	0.60	0.04	0.94	0.38

4. Conclusions

Scour around submarine pipelines under bidirectional tidal currents was investigated by carrying out laboratory 1:20 scale model experiments. The tidal current was simulated as a regular sinusoid tide with various velocities. The temporal development of the scour depth and scour profile characteristics under a bidirectional tidal current are analyzed. The main conclusions can be summarized as follows:

1. Under a bidirectional tidal current, the scour profile, with two dunes on both sides of submarine pipeline, was more symmetric than that subject to a unidirectional current. In addition, the scour width and depth under a bidirectional tidal current were both smaller than those under a unidirectional tidal current.
2. For bidirectional tidal currents, the scour depth increased rapidly during the first half of the tidal cycle. After that, the scour depth only increased slightly when the flow was near maximum flood or ebb tidal velocity, and there was no scour development when flow was close to zero velocity. Additionally, the equilibrium scour depth under a bidirectional current was averagely 0.8 times of that under a unidirectional current whose flow velocity was equal to the maximum tidal velocity.
3. An equation to predict live-bed scour depth around submarine pipelines under bidirectional tidal currents was developed. In this equation, the scour depth under

a bidirectional current was predicted based on a new fitted equation for live-bed scour depth in unidirectional current coupling with a reduction coefficient of 0.8. This equation was used to predict scour depth in practical engineering and showed good agreement with field data, indicating that the present new equation could accurately predict live-bed scour depth around submarine pipelines under bidirectional currents in the field.

Author Contributions: Methodology, Z.Z. and X.W.; data curation, Y.Y.; writing—original draft preparation, Z.Z.; writing—review and editing, Y.G. and B.S. All authors have read and agreed to the published version of the manuscript.

Funding: This study was funded by the Joint Funds of National Natural Science Foundation of China and Shandong Province (Grant No. U2006227), Zhejiang Hydraulic Science and Technology (Grant No. RB1903), Public Welfare Research Project of Zhejiang Province (Grant No. LGF21E090003).

Institutional Review Board Statement: Not applicable.

Informed Consent Statement: Not applicable.

Data Availability Statement: Data from present experiment and field data appear in the submitted manuscript.

Conflicts of Interest: The authors declare no conflict of interest.

Notations

d_{50}	sediment median diameter
D	pipeline diameter
Fr	Froude number
g	gravitational acceleration
h	water depth
d_s	scour depth at $x = 0.0\ D$
d_{sm}	final maximum scour depth
KC	Keulegan–Carpenter number
t	time
T	tidal period
T_w	wave period
u_t	velocity of tidal current at time t
$u_{\max}$	maximum peak velocity of tidal current
u_c	critical velocity for sediment incipient motion
u_0	velocity of unidirectional current
u_{wmax}	peak velocity of wave
x	horizontal direction
z	vertical direction
ρ_s	sediment density
ρ	water density

References

1. Chiew, Y.M. Prediction of maximum scour depth at submarine pipelines. *J. Hydraul. Eng.* **1991**, *117*, 452–466. [CrossRef]
2. Sumer, B.M.; Fredsøe, J. *The Mechanics of Scour in the Marine Environment*; World Scientific Publishing Company: Singapore, 2002.
3. Fredsøe, J. Pipeline–seabed interaction. *J. Waterw. Port Coast. Ocean Eng.* **2016**, *142*, 03116002. [CrossRef]
4. Zhang, Q.; Draper, S.; Cheng, L.; An, H. Scour below a subsea pipeline in time varying flow conditions. *Appl. Ocean Res.* **2016**, *55*, 151–162. [CrossRef]
5. Zhang, Q.; Draper, S.; Cheng, L.; Zhao, M.; An, H. Experimental study of local scour beneath two tandem pipelines in steady current. *Coast Eng. J.* **2017**, *59*, 1750002. [CrossRef]
6. Zhang, Z.Y.; Shi, B.; Guo, Y.K.; Chen, D.Y. Improving the prediction of scour around submarine pipelines. *Proc. Inst. Civ. Eng. -Marit. Eng.* **2016**, *169*, 163–173. [CrossRef]
7. Yang, L.P.; Guo, Y.K.; Shi, B.; Kuang, C.P.; Xu, W.L.; Cao, S.Y. Study of scour around submarine pipeline with a rubber plate or rigid spoiler in wave conditions. *ASCE J. Waterw. Port Ocean Coast Eng.* **2012**, *138*, 484–490. [CrossRef]

8. Yang, L.P.; Shi, B.; Guo, Y.K.; Zhang, L.X.; Zhang, J.S.; Han, Y. Scour protection of submarine pipelines using rubber plates underneath the pipes. *Ocean Eng.* **2014**, *84*, 176–182. [CrossRef]
9. Mao, Y. *The Interaction between A Pipeline and An Erodible Bed*; The Technology University of Denmark: Kongens Lyngby, Denmark, 1986.
10. Chiew, Y.M. Mechanics of local scour around submarine pipelines. *J. Hydraul. Eng.* **1990**, *116*, 515–529. [CrossRef]
11. Kjeldsen, S.P.; Gjorsvik, C.; Bringaker, K.G.; Jacobsen, J. Local scour near offshore pipelines. In Proceedings of the 2nd International Port and Ocean Engineering under Arctic Conditions, Reykjavik, Iceland, 27–30 August 1973; pp. 309–331.
12. Bijker, E.W.; Leeuwestein, W. Interaction between pipelines and the seabed under the influence of waves and currents. In *Seabed Mechanics*; Denness, B., Ed.; Springer: Dordrecht, The Netherlands, 1984; pp. 235–242.
13. Yang, L.P.; Shi, B.; Guo, Y.K.; Wen, X.Y. Calculation and experiment on scour depth for submarine pipeline with a spoiler. *Ocean Eng.* **2012**, *55*, 191–198. [CrossRef]
14. Ibrahim, A.; Nalluri, C. Scour prediction around marine pipelines. In Proceedings of the 5th International Offshore Mechanics and Arctic Engineering, Tokyo, Japan, 13–18 April 1986; pp. 679–684.
15. Moncada-M., A.T.; Aguirre-Pe, J. Scour below Pipeline in River Crossings. *J. Hydraul. Eng.* **1999**, *125*, 953–958. [CrossRef]
16. Cevik, E.; Yuksel, Y. Scour under submarine pipelines in waves in shoaling conditions. *J. Waterw. Port Coast. Ocean Eng.* **1999**, *125*, 9–19. [CrossRef]
17. Lin, Z.B.; Guo, Y.K.; Jeng, D.-S.; Liao, C.C.; Rey, N. An integrated numerical model for wave–soil–pipeline interactions. *Coast. Eng.* **2016**, *108*, 25–35. [CrossRef]
18. Sumer, B.M.; Fredsøe, J. Scour below pipelines in waves. *J. Waterw. Port Coast. Ocean Eng.* **1990**, *116*, 307–323. [CrossRef]
19. Pu, Q.; Li, K.; Gao, F.P. Scour of the seabed under a pipeline in oscillatory flow. *China Ocean Eng.* **2001**, *16*, 129–137.
20. Etemad-Shahidi, A.; Yasa, R.; Kazeminezhad, M.H. Prediction of wave-induced scour depth under submarine pipelines using machine learning approach. *Appl. Ocean Res.* **2011**, *33*, 54–59. [CrossRef]
21. Yasa, R. Prediction of the Scour Depth under Submarine Pipelines—In Wave Condition. *J. Coast. Res.* **2011**, *64*, 627–630.
22. Zhang, J.; Shi, B.; Guo, Y.K.; Xu, W.L.; Yang, K.J.; Zhao, E.J. Scour Development Around Submarine Pipelines due to Current Based on the Maximum Entropy Theory. *J. Ocean Univ. China* **2016**, *15*, 841–846. [CrossRef]
23. Liu, M.M. Numerical investigation of local scour around submerged pipeline in shoaling conditions. *Ocean Eng.* **2021**, *234*, 109258. [CrossRef]
24. Zhang, Q.; Draper, S.; Cheng, L.; An, H. Time Scale of Local Scour around Pipelines in Current, Waves, and Combined Waves and Current. *J. Hydraul. Eng.* **2017**, *143*, 04016093. [CrossRef]
25. Li, Y.; Ong, M.; Fuhrman, D.R.; Larsen, B.E. Numerical investigation of wave plus-current induced scour beneath two submarine pipelines in tandem. *Coast. Eng.* **2020**, *156*, 103619. [CrossRef]
26. Zeng, J.; Chen, G.; Pan, C.; Zhang, Z. Effect of dike line adjustment on the tidal bore in the Qiantang Estuary, China. *J. Hydrodyn.* **2017**, *29*, 452–459. [CrossRef]
27. Ma, L.; Wang, L.; Guo, Z.; Jiang, H.; Gao, Y. Time development of scour around pile groups in tidal currents. *Ocean Eng.* **2018**, *163*, 400–418. [CrossRef]
28. Schendel, A.; Hildebrandt, A.; Goseberg, N.; Schlurmann, T. Processes and evolution of scour around a monopile induced by tidal currents. *Coast. Eng.* **2018**, *139*, 65–84. [CrossRef]
29. McGovern, D.J.; Ilic, S.; Folkard, A.M.; McLelland, S.J.; Murphy, B.J. Time Development of Scour around a Cylinder in Simulated Tidal Currents. *J. Hydraul. Eng.* **2014**, *140*, 04014014. [CrossRef]
30. Zhu, L.; Liu, K.; Fan, H.; Cao, S.; Chen, H.; Wang, J.; Wang, Z. Scour beneath and adjacent to submarine pipelines with spoilers on a cohesive seabed: Case study of Hangzhou Bay, China. *J. Waterw. Port Coast Ocean Eng.* **2019**, *145*, 05018009. [CrossRef]
31. Zhang, R.J.; Xie, J.H.; Wang, M.F. *River Sediment Dynamics*; China Water and Power Press: Beijing, China, 1998.